

Method for Obtaining Shadow Images of Control Objects for Telemetric Care Systems

Lidiia Tereshchenko¹

¹National Aviation University, 1 Lubomyr Huzar ave., Kyiv, 03058, Ukraine

Abstract

The paper deals with two-dimensional spectral detectors for baggage inspection X-ray devices. This detector is based on the construction of analytical models for the internal structure of objects under control and their spectrum calculation. The methods of projective geometry and Bouguer-Lambert law are applied to obtain the analytical models for shadows of three-dimensional objects. Spectral detectors are designed according to the Neyman-Pearson criterion. Analysis shows that the proposed spectral detector has good operating characteristics even at low signal-to-noise ratios.

Keywords

Keywords: aviation security service, X-ray, optical imaging, shadow of three-dimensional objects, spectral detector.

1. Introduction

Ensuring effective protection against terrorism is the most difficult issue, especially for countries with a developed air transport network, a large number of airlines, and airports. The problem is complicated by the unpredictability of terrorists' actions. In addition, vulnerabilities in aviation security systems (such as procedures for screening airline passengers and their baggage, freight shipments, mail, etc.) that can be exploited by law violators should be taken into consideration. The main way to improve aviation safety is to prevent hazardous objects and substances, explosive devices, and weapons on aircraft boards. This requires a comprehensive development and introduction of new methods of screening, detection, and identification of dangerous objects under control. Insights of the direct visualization methods indicate that they are inherent in the same type of operations: primary radiation exposure of the objects under control in configuration space (in the case of active method), reradiation reception (scattered or passed through the object), its conversion into an electrical signal, signal processing and electrical-to-optical signal conversion [1, 2].

2. Problem Statement

The paper addresses applied research challenges concerning the development and application of a new method of determination (visualization) of the internal structure of the Objects Under Control (OC), that enables dangerous OC to be identified with high probability in real-time, increases the speed of dangerous substances identification in luggage, and provides automation of these processes. In addition, the automatic generation of images of hazardous OC allows for periodic inspections of aviation security service operators. Detection systems based on X-ray, computer tomography, and spectroscopy of mobile ions have certain shortcomings [3–9]. Some of these systems can detect well-hidden explosives, but their implementation requires considerable funds. In addition, they have a high level of false alarms (approximately 0.2 ... 0.4). Thus, the development of analytical models for the receipt of multidimensional shadows of translucent objects for further processing will allow the classification of OC, which will greatly facilitate the work of operators serving supervision devices in Aviation Security Service (AvSS), reducing the value of false alarms. Literature analysis showed that the

CPITS 2023: Workshop on Cybersecurity Providing in Information and Telecommunication Systems, February 28, 2023, Kyiv, Ukraine

EMAIL: 10118@ukr.net (L. Tereshchenko);

ORCID: 0000-0001-8183-9016 (L. Tereshchenko);



© 2023 Copyright for this paper by its authors. Use permitted under Creative Commons License Attribution 4.0 International (CC BY 4.0).

CEUR Workshop Proceedings (CEUR-WS.org)

modernization of equipment for AvSS is carried out in two directions: in the part of the improvement of hardware and software. In [10] authors proposed a new X-ray backscatter technique using an un-collimated powerful (high kW) X-ray beam and an efficient pinhole camera encompassed with a high-resolution matrix detector for imaging of an object. Moreover, a high-energy X-ray inspection technique for the reliable inspection of air freight containers was presented in [11]. Analysis of various strategies for object detection in X-ray security imagery is given in [12]. Moreover, the paper [13] also deals with a technique for the classification of X-ray baggage images using convolutional neural networks. The application of deep convolutional neural network as a classification method in medicine X-ray image analysis was considered in [14].

In [15] authors investigated the feasibility of applying straight-line-trajectory-based tomographic imaging configurations to security inspections. The method of automated target recognition with the usage of a reference database, which contains X-ray images of OC, for cargo scanning systems was proposed in [16]. The papers [17, 18] deal with procedures of handguns, shuriken, and razor blades recognition for baggage inspection. The simulation of the internal structure for OC with simple and complex forms using the point source of irradiation in the center, as well as with the bias relative to the center, is considered in [19]. The method developed for optical imaging of the inner structure of the three-dimensional objects allows obtaining a shadow of these objects, exposed to electromagnetic radiation. It has useful applications in different life spheres, such as in medicine, the manufacturing industry, the process of customs supervision of goods and means of transport for commercial use, etc. It allows the AvSS to increase the probability of correct detection of hazardous materials and reduce false alarms in its security system. For medicine, the method may help to increase the probability of health hazard anomaly detection. So aim of this paper is a synthesis of a two-dimensional spectral detector for baggage inspection X-ray devices.

3. Materials and Methods

The construction of an analytical model reduces to the calculation of a projective image of an isotropic object in the case of homogeneous

irradiation by a point source located on the axis of object symmetry perpendicular to the plane of the image (screen). To determine the position of the radiation source, the OC, and the screen with a point source it is appropriate to use the cylindrical coordinate system applied to the Fig. 1. The OC model with complex form is presented in Fig. 2.

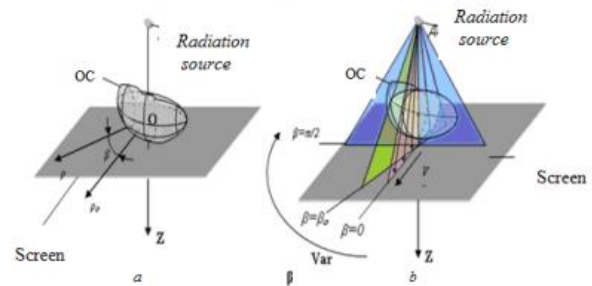


Figure 1: OC scanning: (a) is the setting of a cylindrical coordinate system; (b) is the setting of a scanning beam position

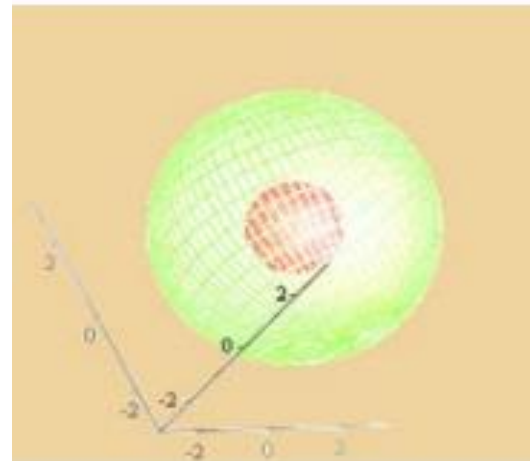


Figure 2: OC with complex form

Internal visualization of the OC with a complex form, in this case, a sphere in the sphere, designed with a point source is shown in Fig. 3.

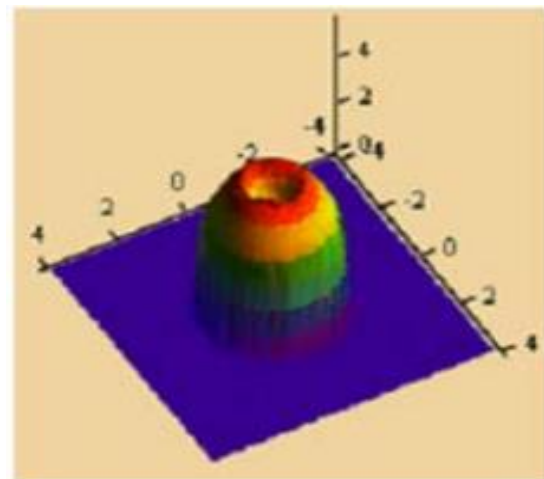


Figure 3: Inner structure imaging for OC

The simulation shows that the simplest objects have shadows with transient characteristics, half-dooms, and distortions of the type of crater, where there are generally flat irradiating planes. Changing the irradiation angle changes the shadow to unrecognizability. To accurately identify the intended OC, it is necessary to automate the process of recognizing shadows, taking into account possible distances between the source, the OC and the screen receiver, the irradiation angles, etc. Methods of analytical modeling of the OC with different shapes, geometrical dimensions, foreshortening, substance, and appropriate extinction coefficients, used to develop procedures for identifying dangerous objects under security supervision of passengers and baggage, allow imaging of OC's inner structure. To verify the developed models multidimensional spectra of visualization images are obtained. The procedure for image processing consists of using a shadow of the object of a given shape to construct a two-dimensional spectrum and its subsequent use in developing the standard spectral detector proposed in the research. This detector is invariant concerning the location of the OC in the working area. The invariance of the calculated spectrum to the location of the OC on the plane of the screen provides the possibility of applying algorithms for the calculation of two-dimensional spatial spectra of the visualization image about the wanted images of some image anomalies in the endoscopic imaging systems of the AvSS. That is, the desired density distribution of the object of control $\mu(x, y)$ must be matched to fit its two-dimensional spatial spectrum—Fourier-image $M(K_x, K_y)$. In the further processing of visualization data, we find solutions in the frequency space $M(K_x, K_y)$, and then, through the inverse Fourier transform, the desired distribution is calculated $\mu^*(x, y)$. The resulting distribution is selected according to those images, which are in the memory of the supervision system. A decision is made to detect a particular object after matching the resulting image $\mu^*(x, y)$ and mask $\mu^*(x, y)$.

Figs. 4 and 5 shows the spectra of images of different shades of opaque OC of a simple shape on the size of a 100×100 screen plane located almost above the center of the screen.

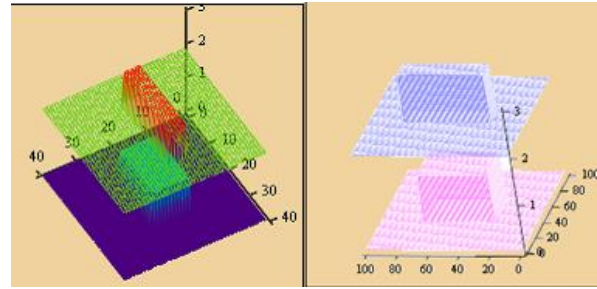


Figure 4: Object of complex shape

Objects marked with stars are not graphs, but drawings illustrating examples of corresponding graphs with the following input data: $k=10$; $a1=2$; $b1=4$; $c1=1$; $d1=1$; $d2=1$; $\alpha1=1$; $a2=1$; $b2=5$; $c2=3$; $\alpha2=1$. The following formulas calculate the imaginary distribution of the visualized parameter with logarithmic gain.

$$b(x, h) = \text{artg} \frac{h}{x}$$

$$X2(x, h) = \sqrt{x^2 + h^2}$$

$$g1 = \text{atg} \left(\frac{b1}{a1} \right)$$

$$g2 = \text{atg} \left(\frac{b2}{a2} \right)$$

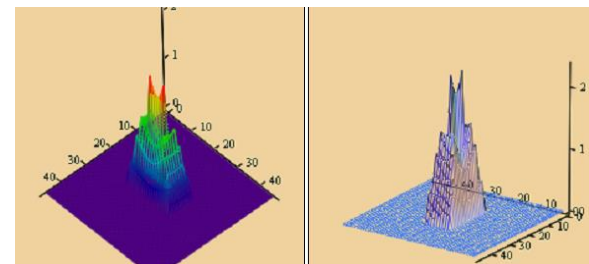


Figure 5: Image of the internal structure of a complex OC with applied parameters in three-dimensional form

Projective image OK with logarithmic gain.

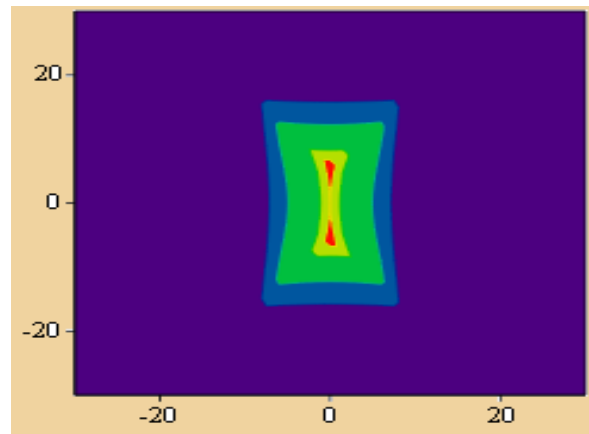


Figure 6: Projective image of OK with logarithmic amplification

The function corresponding to the intensity distribution of the received radiation is obtained by the formula:

$$d(x, h) = e^{-a(x, h)}$$

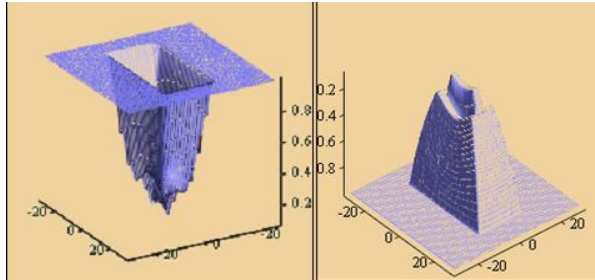


Figure 7: Image of the internal structure of a complex OK with applied parameters, in three-dimensional form

Consider the object of control in the form of a pipe segment with a cavity inside.

Let's set the parameters of the rendering system:

$$r_1 = 3, r_2 = 2, k = 10, d = 1, c = 1, a = 1$$

where k is the distance from the radiation source to the screen; c is the distance from the radiation source to the OK; r_1 is radius OK; r_2 is cavity radius; d is layer thickness; a is the radiation attenuation coefficient in the OK material.

The actual distribution of the extinction coefficient will be:

$$F1(x, y) = \begin{cases} 0 & \text{if } -\sqrt{x^2 + y^2} \leq r_1 \leq \sqrt{x^2 + y^2} \vee (-r_2 < r_2 < -\sqrt{x^2 + y^2} \vee \sqrt{x^2 + y^2} < r_2 < r_1) \\ d & \text{otherwise} \end{cases}$$

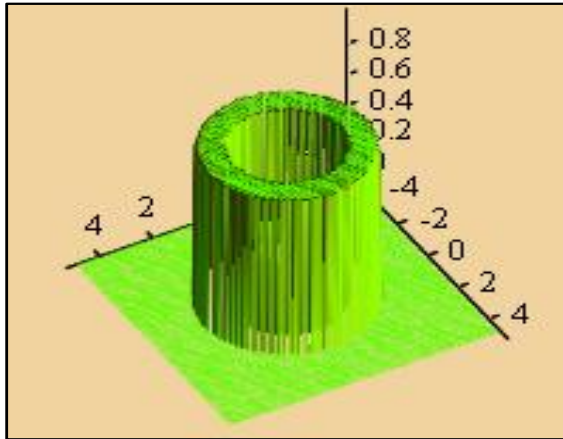


Figure 8: Object

$$OD2 = \frac{r_2 k}{c + d}$$

$$X2(x, h) = \sqrt{x^2 + h^2}, \quad OD2 = \frac{r_2 k}{c + d};$$

$$a(x, h) = (a_p(x, h) - a_v(x, h))a$$

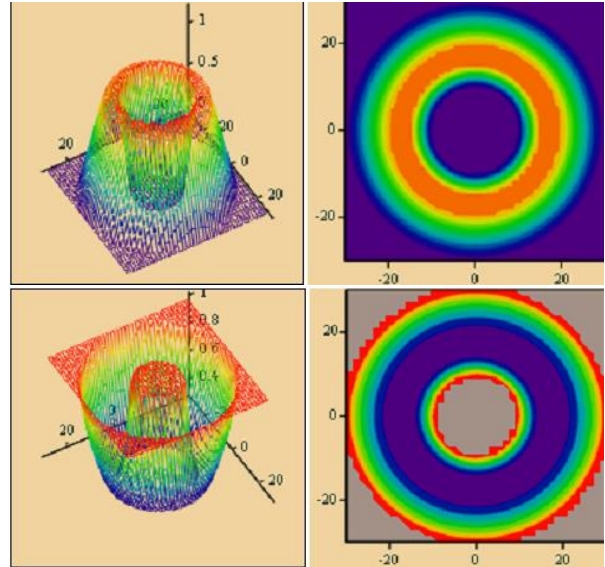


Figure 9: Image of the internal structure of a complex control object with applied parameters, in three-dimensional form

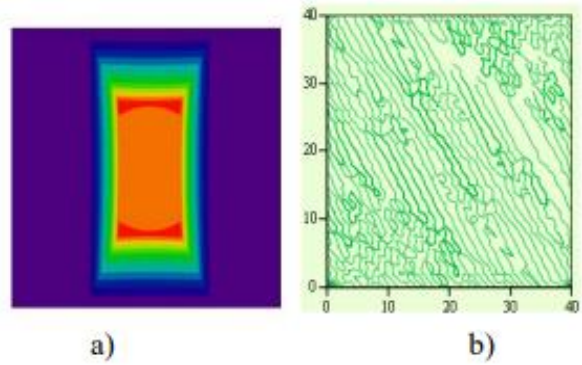


Figure 11: Shadow (a) of a parallelepiped and its spectrum (b)

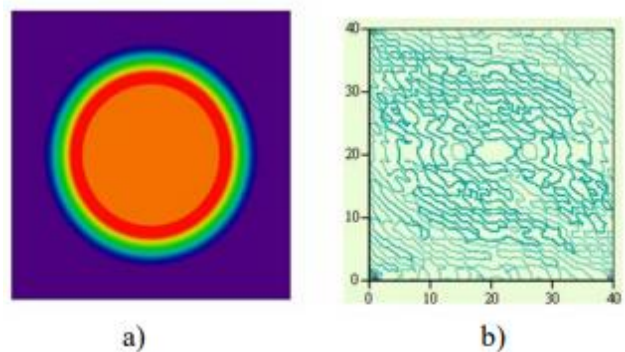


Figure 12: Shadow (a) of the cylinder and its spectrum (b)

On one plane, the shadows of two parallelepipeds are located, and their spectral images are obtained (Fig. 13).

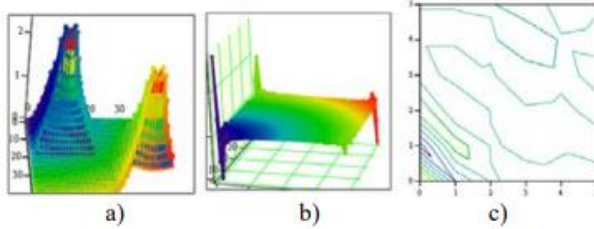


Figure 13: Shadows of two parallelepipeds and their spectrum: a) shadows of two parallelepipeds; b) a three-dimensional image of the spectrum of those shadows; c) a two-dimensional projection of the spectrum of shadows of parallelepipeds

The following figures show the spectral images of the shadows of the parallelepiped and the spheres that were located in space (Fig. 14).

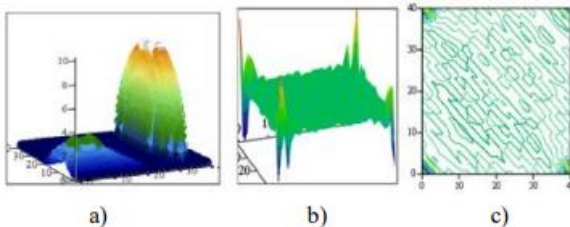


Figure 14: Shadows of parallelepiped and spheres and the spectrum of their compatible shadows: a) shadows; b) a three-dimensional image of the spectrum of those shadows; c) a two-dimensional projection of the spectrum of shadows
Analysis of the spectra of hazardous and forbidden OC allows us to create an appropriate database for the further detection of OC of various shapes and complexity

When using X-ray systems to provide automation of care and increase the reliability of decision-making on the presence of prohibited articles and substances in the OC, there are problems in identifying different forms and locations of the OC. For this purpose, the example of the spectral detector model was constructed in the Matlab environment. In this case, the detection occurs regardless of the OC location and regardless of its shape and size. The considered models are the shadows of two objects in a field with specified boundaries. One object is a regular square (this kind can have dynamite), and the other is a model of the machine gun (Fig. 15). Also, white Gaussian noise and a mixture of image and noise are modeled (Fig. 16). The developed program allows us to detect an OC with a given probability of false alarms for the corresponding threshold decision depending on the size of the OC. The program calculates the

probability of correct detection of a signal from an OC.

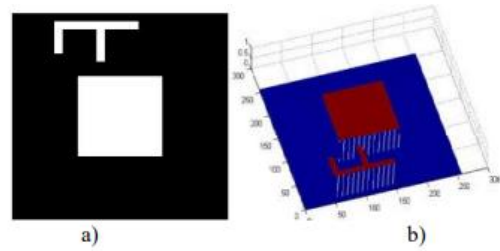


Figure 15: Model of shadow OC

A mixture of useful signals and noise is shown in Fig. 15. A mixture of signal with noise in cases of signal-to-noise ratios equaled to 2 (a) and 0.5 (b) The Neyman-Pearson criterion is applied for optimal detection of an OC. According to the Neyman-Pearson criterion, the threshold level V is determined from the condition that the probability of a correct detection D with the given probability of false alarm F was maximal. Hence, the optimal character of the Neyman-Pearson criterion is that it maximizes the probability of correct detection at a fixed probability of false alarms. In addition, it should be noted that the program calculates the characteristics of the detection. An example of these characteristics is shown in Fig. 10. On these graphs it is seen that when the decision threshold is reduced, the detection characteristic is more efficient, however, the probability of false detection is increased. The analysis shows that the developed spectral detector has good detection characteristics even at low signal-to-noise ratios.

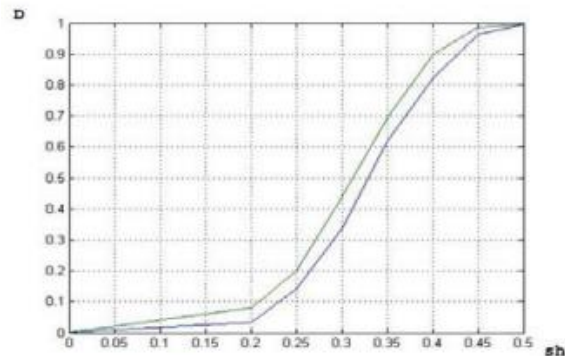


Figure 16: Characteristics of signal detection for sample size 1000 and probabilities of false alarms $F = 0.05$ and $F = 0.03$

4. Conclusions

The analysis of scientific publications has shown that the most effective methods for the detection and identification of hazardous OCs are

transient multi-energy direct X-ray ones. They provide reliable detection of hazardous OCs. However, these methods are complicated, their implementation in the supervisory systems has a significant expenditure of material resources, and they do not work efficiently with dynamic OCs. At a high probability of correct detection to 0.99, there is a high probability of false alarms from 0.3 to 0.4. The simulation shows that the simplest OC has shadows with transient characteristics, half-dooms, and distortions of the type of crater, where there are generally flat irradiating planes. Changing the irradiation angle changes the shadow to unrecognizability. To accurately identify the intended OC, it is necessary to automate the process of recognizing shadows, taking into account possible distances between the source, the OC and the screen receiver, the irradiation angles, etc. The procedure for image processing consists of using a given shape OC shadow to construct a two-dimensional spectrum and its subsequent use in developing the standard spectral detector. This detector is invariant concerning the location of the OC in the working area. To solve the problem, a spectral detector model is developed using the MatLab software environment. In this case, the detection occurs regardless of the OC location or its shape and size. It allows the detection of dangerous objects with a high probability of correct detection and a low probability of false positives (from 0.03 to 0.05).

5. References

- [1] K. Khorolska, et al., Application of a Convolutional Neural Network with a Module of Elementary Graphic Primitive Classifiers in the Problems of Recognition of Drawing Documentation and Transformation of 2D to 3D Models, *Journal of Theoretical and Applied Information Technology* 100(24) (2022) 7426–7437.
- [2] Z. B. Hu, et al., Authentication System by Human Brainwaves Using Machine Learning and Artificial Intelligence, in: *Advances in Computer Science for Engineering and Education IV* (2021) 374–388. doi: 10.1007/978-3-030-80472-5_31
- [3] O. Semenov, *Theoretical Foundations and Principles of Construction of Technical Devices for Aviation Security: Training Guide*, Kyiv, NAU, 2001, 214.
- [4] S.Kolkoori, N. Wrobel, U. Ewert, A new X-Ray Backscatter Technology for Aviation Security Applications, *IEEE International Symposium on Technologies for Homeland Security (HST)*, Waltham, MA, USA, April 2015, 1–5. doi:10.1109/THS.2015.7225329
- [5] S. Kolkoori, et al., High Energy X-Ray Imaging Technology for the Detection of Dangerous Materials in Air Freight Containers, *IEEE International Symposium on Technologies for Homeland Security (HST)*, Waltham, MA, USA, April 2015, 1–6.
- [6] S. Akcay, T. Breckon, An Evaluation of Region Based Object Detection Strategies Within X-Ray Baggage Security Imagery, *IEEE International Conference on Image Processing (ICIP)*, Beijing, China, September 2017, 1337–1341.
- [7] S. Akcay, et al., Transfer Learning Using Convolutional Neural Networks for Object Classification Within X-Ray Baggage Security Imagery, *IEEE International Conference on Image Processing (ICIP)*, Phoenix, AZ, USA, September 2016, 1057–1061.
- [8] K. Kurachka, I. Tsalka, Vertebrae Detection in X-Ray Images Based on Deep Convolutional Neural Networks, *IEEE 14th International Scientific Conference on Informatics*, Poprad, Slovakia, November 2017. doi:10.1109/informatics.2017.8327245
- [9] H. Gao, et al., Straight-Line-TrajectoryBased X-Ray Tomographic Imaging for Security Inspections: System Design, Image Reconstruction and Preliminary Results, *IEEE Transactions on Nuclear Science*, 60(5) (2013) 3955–3968. doi:10.1109/tns.2013.2274481
- [10] W. Visser, et al., Automated Comparison of X-ray Images for Cargo Scanning, *IEEE International Carnahan Conference on Security Technology (ICCST)*, Orlando, FL, USA, October 2016, 1–8. doi:10.3390/s21217294
- [11] D. Mery, A. Katsaggelos, A Logarithmic X-ray Imaging Model for Baggage Inspection: Simulation and Object Detection, *IEEE Conference on Computer Vision and Pattern Recognition Workshops*, Honolulu, HI, USA, July 2017, 251–259.
- [12] C. Meghare, C. Gode, Automated Detection of Threat Object in X-ray Images of Baggage, *International Journal of Electrical, Electronics and Data Communication*, 5(6) (2017), 97–101.

- [13] A. Semenov, L. Tereshchenko, Modeling of the Visualization of the Internal Structure of Objects of Control, *Electronics and Control Systems*,1 (2008) 144–148.
- [14] S. Cusick, A. Cortes, C. Rodrigues, *Commercial Aviation Safety*, Sixth Edition, New York: McGraw-Hill Education, 2012, 696.
- [15] *Safety Management Manual*. Montreal: International Civil Aviation Organization, 2018.
- [16] M. Chen, Y. Zhang Y. Chen, Review on Civil Aviation Safety Investment Research, 11th International Conference on Reliability, Maintainability and Safety (ICRMS), 2016, 1–5. doi:10.1109/ICRMS.2016.8050113
- [17] M. Zaliskyi, et al., Method of Traffic Monitoring for DDoS Attacks Detection in E-Health Systems and Networks, *CEUR Workshop Proceedings*, 2255 (2018) 193–204.
- [18] M. Shutko, et al., Two-Dimensional Spectral Detector for Baggage Inspection X-Ray System, *CEUR Workshop Proceedings* 2300 (2018) 63–66.
- [19] M. Zaliskyi, et al., Shadow Image Processing of X-Ray Screening System for Aviation Security, *International Journal of Image, Graphics and Signal Processing (IJIGSP)* 14 (6) (2022) 26–46. doi:10.5815/ijigsp.2022.06.03